

1 Supplementary Information

2

3

4 **Vegetation recovery in tidal marshes reveals critical slowing down under** 5 **increased inundation**

6

7 *Jim van Belzen, Johan van de Koppel, Matthew L. Kirwan, Daphne van der Wal, Peter M.J.*

8 *Herman, Vasilis Dakos, Sonia Kéfi, Marten Scheffer, Glenn R. Guntenspergen & Tjeerd J.*

9 *Bouma*

10

11

12 **Supplementary Note 1: Critical slowing down in a simple tidal marsh model**

13 *Model description*

14 We developed a simple spatially explicit tidal marsh model adding on ref. [1] to
15 investigate how critical slowing down manifests along the environmental stress gradient
16 elevation due to inundation by seawater. We applied a minimal modelling approach in that
17 we included only those aspects relevant for information of tidal marsh along the inundation
18 gradient, focusing on the coupling of vegetation and sediment elevation. The full model
19 describes changes in vegetation density and elevation along the gradient from land towards
20 the sea by the following partial differential equations:

$$21 \quad \frac{\partial V}{\partial t} = r \frac{z}{z+a} \left(1 - \frac{V}{K}\right) V - m \frac{b}{V+b} \tau(x) V + d_V \Delta V \quad (1)$$

$$22 \quad \frac{\partial z}{\partial t} = S_{max} \left(1 - \frac{z}{z_{max}}\right) - e_{max} \frac{c}{V+c} \tau(x) z + d_z \Delta z \quad (2)$$

23 Here, V and z are the vegetation density (g m^{-2}) and elevation (m) respectively and are
24 functions of position x and time t . The model assumes logistic growth of the tidal marsh
25 vegetation where r is the maximum growth rate (d^{-1}) and K the maximum standing crop of
26 the vegetation (g m^{-2}). The term $(z/z+a)$ is included to account for the positive effect of
27 elevation (higher elevation is lower inundation time) on growth, where a is the elevation at
28 which growth is reduced by half. The vegetation is further hampered due to hydrodynamic
29 forcing, such as waves and tidal currents, which increase in importance from the land to the
30 seaward edge of the tidal marsh. We included this as a standardized bottom shear stress
31 $\tau(x)$, which is 0 at the landward and 1 at the seaward edge. The maximum loss rate of the
32 vegetation due to hydrodynamic forcing is m (d^{-1}). As the effect of hydrodynamic forcing on
33 the loss of vegetation is density-dependent the term $(b/(V+b))$ is included. At high densities,
34 loss of vegetation is reduced due to attenuation and divergence of hydrodynamic energy^{1,2}
35 explaining why single seedlings or small tussocks of vegetation on a bare mudflat have little
36 chance of survival^{3,4}. The amelioration effect by the vegetation is half maximal at density b .
37 Furthermore, we added lateral dispersal of V from and to neighboring sites due to
38 colonization via rhizomes, at rate d_V .

39 The development of the elevation z is determined by sedimentation, erosion and
40 some lateral sediment fluxes. Net deposition is determined by the maximum deposition S_{max}
41 ($m\ d^{-1}$), the elevation z (m) and the maximum elevation z_{max} (m) that represents the
42 astronomical high water level the tidal marsh experiences. Simply put, higher elevations are
43 less long inundated by seawater and thus sediments are deposited for shorter period
44 reducing the rate at which the elevation accretes. Sediments can erode due to
45 hydrodynamic forcing along the gradient of bottom shear stress $\tau(x)$ at a maximum E_{max} (d^{-1}).
46 Here, vegetation can reduce erosion e.g. due to attenuation of waves and tidal currents.
47 Erosion is reduced by half at the vegetation density c . Furthermore, there is some diffusive
48 lateral sediment exchange due to e.g. gravity at rate d_z .

49 Parameter values were obtained from our field experiments, personal observations
50 and literature of similar models^{1,4}. The parameter values used for the model analysis were: r
51 $= 2.7*10^{-3}\ day^{-1}$, $K = 1000\ g\ m^{-2}$, $a = 1\ m$, $m = 2.19*10^{-3}\ day^{-1}$, $b = 250\ g\ m^{-2}$, $d_v = 0.012\ m^2$
52 day^{-1} , $S_{max} = 14*10^{-5}\ m\ day^{-1}$, $z_{max} = 4\ m$, $e_{max} = 41*10^{-5}\ day^{-1}$, $c = 250\ g\ m^{-2}$ and $d_z = 0.012\ m^2$
53 day^{-1} .

54 Estimates for r , K and a were based on our experiments and literature^{1,5}. The values for S_{max} ,
55 and e_{max} were derived from ref. [1]. All other parameters were based on similar parameters
56 reported in refs. [1-2].

57 Tidal marsh dynamics were simulated along a 1000 m long cross-shore profile, with
58 0.25 m discrete sites. The model was initialized by allowing the elevation to reach an
59 equilibrium height without the influence of vegetation (the initial bare tidal flat). This
60 became reference elevation z_0 . Next, vegetation is allowed to grow and colonize the bare
61 tidal flat for 100 years before the perturbation experiments are simulated. The new
62 elevation and vegetation density, z_1 and V_1 respectively, serve as a second reference.

63 *Measuring Critical Slowing Down in the model*

64 We focused on how Critical Slowing Down manifests along the environmental stress
65 gradient in the tidal marsh model, comparable to the disturbance-recovery experiments in
66 the field and the time series analysis of the aerial photographs. First we remove 50% of the
67 vegetation biomass of a site to simulate a clipping disturbance. We let the vegetation
68 recover for 100 days (Δt), after which the recovered biomass V_{rec} was obtained.

69 To simulate the natural disturbance-recovery dynamics due to the erosion of
70 vegetation patches we removed 100% of the vegetation and the elevation was reduced to
71 z_0 . We let the vegetation recover for 10 years (Δt). The recovery rates are calculated as (see
72 Supplementary Note 2):

$$73 \quad \lambda = -\log((1 - f)/d)/\Delta t \quad (3)$$

74 Here f is the relative recovery defined as V_{rec}/V , and d is the magnitude of the vegetation
75 disturbance (here 0.5 for the clipping disturbance and 1 for the erosion disturbance). After a
76 disturbance-recovery experiment is simulated, the procedure is repeated from the
77 initialized vegetation density and elevation (V_1 and z_1) values moving to the next site. The

78 obtained recovery rates are interpreted using the initial unvegetated elevation z_0 as
79 explanatory variable as this is a proxy for the inundation time.

80 *Simulated results*

81 The model results support that Critical Slowing Down can be found along the
82 elevation gradient (Supplementary Figure 2). For both types of disturbance-recovery
83 experiments we found that the recovery rates decrease from high to low elevations, like we
84 found in our empirical data, and consistent with Critical Slowing Down. Like in our empirical
85 data, the recovery rates of our clipping experiment are a magnitude higher than the
86 recovery from erosion disturbances. These results reveal that tidal marsh resilience differs
87 markedly depending on the type of disturbance, but still in a consistent way along the main
88 stress gradient. Thus, based on the main governing processes modelled in this simple model
89 we can expect Critical Slowing Down to occur along the elevation gradient in real life cases.

90

91

92 **Supplementary Note 2: Measuring recovery rates from experimental data**

93 Measuring recovery rates to reliably estimate the resilience in real-world tidal-marsh
94 systems is challenging due to e.g.: 1) difficulty in getting frequent field observations of
95 biomass; 2) seasonal dynamics; and of 3) the high level of heterogeneity and stochasticity in
96 the intertidal system. These above points pose some serious challenges to the usual
97 approach for estimating the recovery rates in perturbed systems. Here, we describe
98 which approaches were used in this study to deal with these issues and obtain reliable
99 estimates on the resilience of vegetation in the field.

100 Most theoretical and empirical studies follow the nondestructive monitoring
101 approach proposed by ref. [6] for estimating the recovery rate, λ . Here, an exponential
102 model is fitted against the time series of the biomass development that is obtained of the
103 recovery after the disturbance. In the empirical studies that tested resilience indicators so
104 far (e.g. ref. [7, 8]) the state of the system could be relatively easily tracked without
105 disturbing the biomass. For instance, in ref. [7] the researchers used the light attenuated as
106 a proxy for the biomass. By measuring the light attenuation in the mesocosm frequently and
107 at regular intervals the changes in biomass could be tracked; Likewise, in ref. [8] the
108 concentration of cells could be monitored without disturbing the cell numbers. A second
109 method, often used in simulation studies, is to measure the time it takes before the system
110 is recovered to the pre-disturbed state (e.g. used in ref. [9]). The biomass has to be
111 recovered within a certain accuracy around the pre-disturbed value (e.g. within 0.01 or
112 0.05%) before the disturbance-recovery experiment is stopped.

113 These approaches are, however, impractical for the assessment of resilience of
114 vegetation in the field. The first methodology (i.e. monitoring of biomass development)
115 requires a series of observations about the vegetation development after disturbance.
116 Tracking biomass (i.e. vegetation) development frequent and at regular intervals is
117 particularly challenging due to the nature of the intertidal environment and the accuracy of
118 the available methods to do so. Due to the tides, accessibility of the field sites shifts from
119 day to day, and from one week to the other, making recurrent field visits logistically difficult.
120 Biomass measures, such as canopy height or coverage are impractical, laborious and can be
121 inaccurate at the small scale of the disturbances due to the high level of variability.
122 Automated observations, e.g. with fixed camera's, still need extensive calibration and might
123 suffer from the harsh hydrodynamic conditions and biofouling. For the second methodology
124 (i.e. monitoring of recovery time) all the above objections remain and are supplemented
125 with the fact that the duration of the experiments is determined by the recovery time,
126 which is impractical. Therefore, an alternative and easy to execute method was required.

127 To circumvent the above issues, we measured the recovery rate using destructive
128 sampling approach after a fixed time interval consecutive to the disturbance and compared
129 the recovery in the disturbed plot with a proxy for the equilibrium biomass, V_{eq} . This
130 approach is comparable with measuring net primary productivity over a certain time
131 interval (Δt). Like ref. [6], we assume that during the recovery period the development
132 approximates an inverse exponential:

$$133 \quad V(t) = V_{eq} - V_{eq}De^{-\lambda t} \quad (4)$$

134 Here, $V(t)$ is the biomass at time t , V_{eq} is the equilibrium biomass, and D the disturbance as
135 the amount of biomass removed. To find the recovery rate λ after a fixed time interval Δt
136 we can normalize the function if we define the relative recovery f as $V(\Delta t)/V_{eq}$. In that case
137 the equation writes as:

$$138 \quad f = 1 - de^{-\lambda \Delta t} \quad (5)$$

139 in which d is the relative disturbance magnitude, as D/V_{eq} . This leads to the derivation of the
140 recovery rate λ in equation 3.

141 Finally, we solved the problem that the high level of heterogeneity and stochasticity
142 in the intertidal system poses for the estimation of an equilibrium biomass to which the
143 recovery measurements are related. Due to the high variability of biomass in the field in
144 both the control as well as the experimental plots, pairing them leads to odd results. For
145 instance, this can lead to >100% recovery, which makes it impossible to estimate the
146 recovery rate. However, if we assume that both the control as the experimental plots are
147 sufficiently independent (which is corroborated by the high variability between plots) we
148 can estimate the vegetation distribution parameters (i.e. mean and standard deviation).
149 Therefore, a proxy of equilibrium vegetation V_{eq} was based on the estimate of the maximum
150 biomass of the vegetation per elevation level. This was estimated as the mean biomass of
151 the controls at an inundation level plus 3 times the standard deviation (i.e. the three-sigma-
152 rule).

153 A full protocol for the disturbance-recovery experiments can be found in ref [10].

154

155

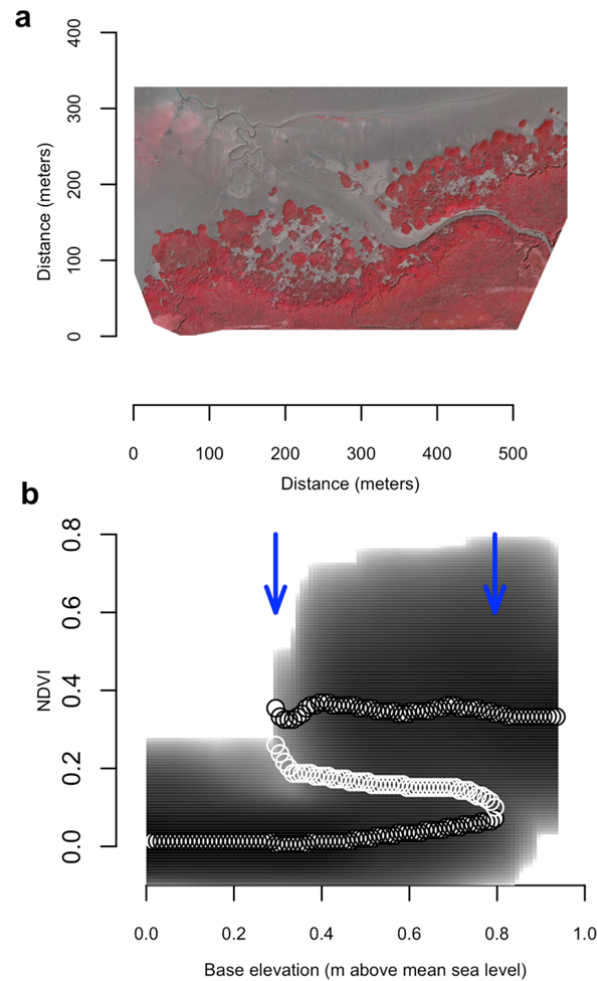
156

157

158 **Supplementary References**

- 159 1. van de Koppel, J., van der Wal, D., Bakker, J.P., Herman, P.M.J. Self-organization and
160 vegetation collapse in salt marsh ecosystems. *Am. Nat.* **165**, E1-12 (2005)
- 161 2. Bouma, T.J. *et al.* Density-dependent linkage of scale-dependent feedbacks: a flume
162 study on the intertidal macrophyte *Spartina anglica*. *Oikos* **118**, 260-268 (2009)
- 163 3. van Wesenbeeck, B.K., van de Koppel, J., Herman, P.M.J., Bouma, T.J. Does scale-
164 dependent feedback explain spatial complexity in salt-marsh ecosystems? *Oikos* **117**,
165 152-159 (2008)
- 166 4. Schwarz, S. *et al.* Abiotic factors governing the establishment and expansion of two
167 salt marsh plants in the Yangtze estuary, China. *Wetlands* **31**, 1011-1021 (2013)
- 168 5. Temmerman, S., Bouma, T. J., Govers, G., Lauwaert, D. Flow path of water and
169 sediment in a tidal marsh: Relations with marsh developmental stage and tidal
170 inundation height. *Estuaries* **28**, 338-352 (2007).
- 171 6. Van Nes, E. H. & Scheffer, M. Slow recovery from perturbations as a generic indicator
172 of nearby catastrophic shift. *Am. Nat.* **169**, 738-747 (2007).
- 173 7. Veraart, A. J. *et al.* Recovery rates reflect distance to a tipping point in a living
174 system. *Nature* **481**, 357-359 (2012).
- 175 8. Dai, L., Vorselen, D., Korolev, K. S. & Gore, J. Generic indicators for loss of resilience
176 before a tipping point leading to population collapse. *Science* **336**, 1175–1177
177 (2012).
- 178 9. Dakos, V., Kéfi, S., Rietkerk, M., van Nes, E. H., & Scheffer, M. Slowing down in
179 spatially patterned ecosystems at the brink of collapse. *Am. Nat.* **177**, E153-E166
180 (2011).
- 181 10. van Belzen, J, van de Koppel, J, Kirwan, M.L, Guntenspergen, G.R, Bouma, T.J.
182 Disturbance-recovery experiments to assess resilience of ecosystems along a stress
183 gradient *Protocol Exchange* doi:10.1038/protex.2017.028 (2017)

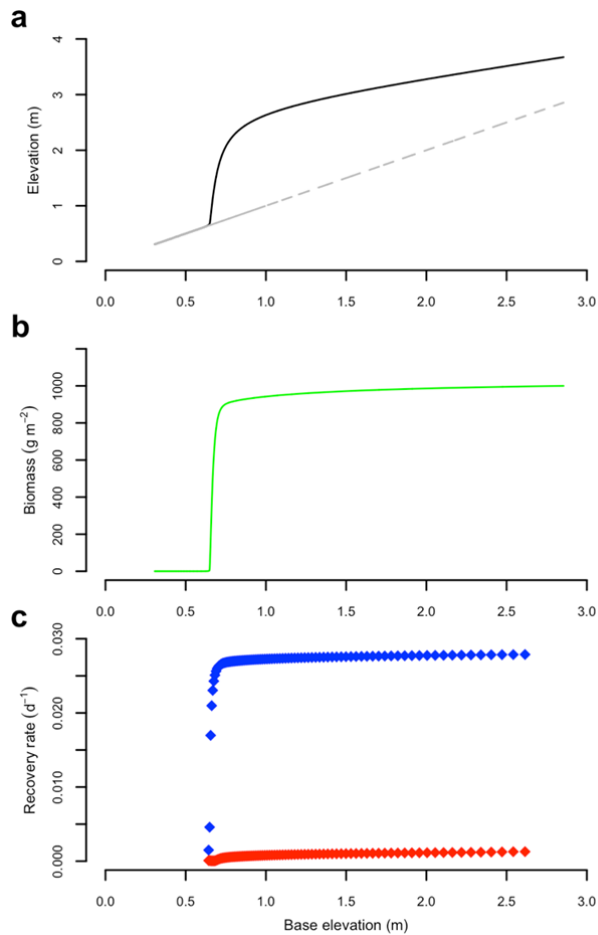
184
185
186
187
188



190

191 **Supplementary Figure 1 | The tidal marsh, and bimodality of vegetation along an**
 192 **environmental stress gradient of seawater inundation.**

193 **(a)** False color image of tidal marsh vegetation along inundation gradient (red indicates
 194 vegetated area) from the sea to land side. **(b)** Reconstruction of the potential (dark gray
 195 shading) of the vegetation along the inundation gradient based on the Normalized
 196 Difference Vegetation Index (NDVI) suggest the possibility of tipping points in this tidal
 197 marsh. The reconstruction indicates a region of bimodality at intermediate inundation times
 198 between the high NDVI (biomass) tidal marsh state and a low NDVI (biomass) tidal flat state.
 199 White filled and open dots depict these local minima and maxima respectively. Blue arrows
 200 depict the critical conditions of marsh vegetation. Panels are based on data from site 2
 201 'Paulina'.
 202



203

204

Supplementary Figure 2 | Tidal marsh development and critical slowing down in a simple model.

205

206

(a) The equilibrium elevations that establishes along the cross-shore profile in the model.

207

Without vegetation a lower base elevation establishes (dashed grey line) and within the

208

vegetated part of the mudflat the elevation is increased (solid black line). **(b)** Biomass

209

pattern (green line) along the cross-shore profile shows sudden rise in biomass coinciding

210

with the deviating elevation from the base elevation. **(c)** Recovery rates from a simulated

211

clipping disturbance (blue dots) and erosion disturbance (red dots) decrease from high to

212

low elevation indicating critical slowing down.

213

214

215 **Supplementary Tables**

216 **Supplementary Table 1 | Data available and used of Dutch study sites**

year	False Color Composite of aerial images	Bathymetry
1976	1	
1982	1, 2	1*, 2*
1992		1*, 2*
1993	1	1*, 2*
1994		1*, 2*
1996	1, 2	1#, 2#
1997		1#, 2#
1998	1, 2	1#, 2#
2001	1, 2	1, 2
2004	1	1, 2
2008	1, 2	1, 2
2010	1, 2	1, 2
2011	1, 2	?
2012	1, 2	?

1) site 1, Hellegat; 2) site 2, Paulina; *) only data of channels; #) only data of tidal flat adjacent to marsh

217

218

219 **Supplementary Table 2 | Correlation between average inundation time and measured**
 220 **indicators of tidal marsh resilience**

	Parameter	site 1 Hellegat		site 2 Paulina		site 3 Chesapeake: Blackwater	
		r	P	r	P	r	P
Remote sensing	Coverage (%)	-0.79	<0.001*	-0.97	<0.001*		
	Recovery rate (d ⁻¹)	-0.91	<0.001*	-0.77	<0.005*		
	Variance	0.71	<0.001*	0.02	0.96		
	Neighborhood correlation	0.77	<0.001*	0.44	0.13		
Field experiment	Dry mass (g m ⁻²)	-0.95	<0.001*	-0.10	<0.001*	-0.33	<0.001*
	Recovery rate (d ⁻¹)	-0.43	0.02*	-0.53	<0.005*	-0.81	0.008*

* Pearson's r values are significant

221

222

223 **Supplementary Table 3 | Sensitivity of resilience indicators for the spatial resolution**

Spatial indicator	Site	Spatial resolution							
		0.25 m		1 m		5 m		10 m	
		r	P	r	P	r	P	r	P
Variance	#1 Hellegat	0.71	<0.001*	0.73	<0.001*	0.71	<0.001*	0.69	<0.001*
	#2 Paulina	0.02	0.96	0.22	0.47	0.25	0.40	0.24	0.42
Neighborhood correlation	#1 Hellegat	0.77	<0.001*	0.78	<0.001*	0.76	<0.001*	0.76	<0.001*
	#2 Paulina	0.44	0.13	0.49	0.09	0.46	0.11	0.36	0.22

* Pearson's r values are significant

224

225

226